[32]P. M. Morse, L. A. Young, and E. S. Haurwitz, Phys. Rev. 48, 948 (1935).

[33]R. H. Garstang, Proc. Cambridge Phil. Soc. 52, 107 (1956).

[34]C. Nicolaides and O. Sinanoğlu, Phys. Letters 33A, 178 (1970).

[35]By "HF sea" (of the first row) we mean the set of $1s$, $2s$, $2p$ spin orbitals whether occupied or unoccupied.

[36]N. W. Winter, A. Laferriere, and V. McKoy, Phys. Rev. A 2, 49 (1970).

[37]G. H. Shortley, Phys. Rev. 57, 225 (1940).

[38]E. U. Condon and G. H. Shortley, *The Theory of Atomic Spectra* (Cambridge U. P., Cambridge, England, 1967), p. 253. For the $^2D_{3/2}$-$^2P_{3/2}$ line, the coefficient of H^2 on p. 253 is apparently in error. It should give a numerical answer 288 instead of 1458.

[39]H. F. King, R. E. Stanton, H. Kim, R. E. Wyatt, and R. G. Parr, J. Chem. Phys. 47, 1936 (1967).

[40]This method, based on the corresponding orbital transformation of Amos and Hall [Proc. Roy. Soc. (London) A263, 483 (1961)], shows how any two sets of spin orbitals F_i and F_j can be transformed into equivalent sets of $\hat{F}_i$ and $\hat{F}_j$ such that their overlap matrix is diagonal, i.e.,

$$\langle \hat{F}_i \mid \hat{F}_j \rangle = D_{ii}\delta_{ij}.$$

[41]P. S. Kelly, Astrophys. J. 140, 1247 (1964); J. Quant. Spectry. Radiative Transfer 4, 117 (1964).

[42]In previous work (Ref. 23), where the effect of spin-orbit interaction on forbidden lines was examined, the line strengths S_Q were expressed in terms of s_q [Eq. (3) of text] and a parameter $\chi = \frac{1}{5}(\zeta/F_2)$, where ζ is the spin-orbit parameter and F_2 is the Slater integral. For example, for O I $^1S_0$-$^1D_2$, $S_Q = \frac{20}{3}\, s_q^2(1 + \frac{7}{24}\chi^2 + \cdots)$. The parameter χ is taken as a measure of the departure from pure LS coupling (being 0 for pure LS and ∞ for pure jj coupling). For the ions considered, the magnitude of χ^2 is of order 10^{-4} and therefore its additive effect on the line strengths is negligible.

[43]C. C. J. Roothaan and P. S. Kelly, Phys. Rev. 131, 1177 (1963).

[44]C. Froese, Astrophys. J. 145, 932 (1966).

[45]The matrix elements for the magnetic dipole transition operator $(\vec{L}+2\vec{S})$ are given exactly by group theory. The calculation of magnetic dipole-transition probabilities involve the details of the wave functions only in the evaluation of the spin-orbit, spin-spin, and spin-other-orbit parameters in terms of which the coefficients in intermediate coupling are expressed. All three interactions have been considered in the calculations of Ref. 20. Improvement of the three parameters through the use of N-electron wave functions should change the transition probability only slightly. Therefore we consider the value $A(2972) = 0.067$ sec^{-1} quite accurate with a possible $\pm 5\%$ error.

[46]O. Sinanoğlu, Comments At. Mol. Phys. 2, 79 (1970).

[47]W. L. Wiese, M. W. Smith, and R. M. Glennon, *Atomic Transition Probabilities*, Natl. Bur. Std. (U.S.) (U.S. GPO, Washington, D. C., 1966), Vol. 1.

[48]R. Steele and E. Trefftz, J. Quant. Spectry. Radiative Transfer 6, 833 (1966).

[49]B. H. Armstrong and K. L. Purdum, Phys. Rev. 150, 51 (1966).

PHYSICAL REVIEW A VOLUME 4, NUMBER 4 OCTOBER 1971

Correlation Energy of the Neon Atom*

Taesul Lee, N. C. Dutta, and T. P. Das
Department of Physics, University of Utah, Salt Lake City, Utah 84112

(Received 21 January 1971)

The linked-cluster many-body perturbation theory has been applied in a calculation of the correlation energy of the neon atom in the ground state (^1S). The pair-correlation energy, obtained by summing the correlation energy between all pairs of states in the atom, is found to be $-0.413\,26$ a.u. About 5% of the pair-correlation energy comes from excitations to g, h, and i states. Pair-pair interactions are found to be important and contribute $0.022\,44$ a.u. to the correlation energy. Correlation diagrams involving simultaneous excitations of three and more particles are found to be relatively unimportant and lead to a net contribution of only about 0.003 a.u. Our final value for the correlation energy is $-0.389\,14$ a.u., which is in excellent agreement with the nonrelativistic experimental correlation energy of -0.389 a.u. A detailed comparison is made with the available configuration interaction calculations both with respect to numerical results as well as to the relative importance of various physical effects which contribute to the correlation energy.

I. INTRODUCTION

The study of many-body effects in atomic systems is currently in an accelerated state of development judging by the increasing number of publications in this field and the variety of atomic properties for which many-body effects are being analyzed. The procedures in most frequent use at the present time can be classified broadly under two categories: variational and perturbation types. All the current variational approaches for atoms with more than two or three electrons use the con-

figuration interaction (CI) procedure, and attempts have been made to classify the configurations in a manner representative of the relative importance of two-, three-, and more-particle contributions. In the perturbation method, referred to as LCMBPT (linked-cluster many-body perturbation theory), one utilizes the linked-cluster expansion developed by Brueckner[1] and Goldstone.[2] The various terms in the perturbation series are classified according to diagrams which are evaluated using a complete set of basis states.

In some of the articles on the CI procedure, comments have been made about the need to establish detailed contact between the CI and LCMBPT procedures, particularly with respect to the descriptions of various many-body effects in the two procedures. A beginning in this direction, beyond qualitative analysis, has been made by Lyons and Nesbet,[3,4] who made a quantitative comparison between the contributions to the hyperfine constant from the contact, orbital, and dipolar terms in the lithium atom in the excited ^2P state. A detailed CI calculation of the hyperfine structure (hfs) constant in boron (^2P) has also been reported recently[5] by Nesbet and attempts[6] are under way using the LCMBPT procedure to make a detailed comparison with the various types of many-body contributions obtained by Nesbet.

One aim of the present paper is to make an accurate calculation of the correlation energy in neon using the LCMBPT procedure. A related calculation on the isoelectronic hydrogen fluoride molecule has recently been reported.[7] The second aim is to make a detailed identification of the contributions from classes of diagrams in the LCMBPT procedure with classes of configurations in the CI procedure. Neon is in fact a rather good example for attempting such a comparison for two broad reasons. First, it is a simple enough system so that one does not require an inordinate amount of computational effort to obtain contributions to the correlation energy to a high degree of precision. Yet, it is complicated enough with three shells ($1s$, $2s$, and $2p$) to allow one to make definitive conclusions about the importance of intershell and intrashell correlations.

The second reason for choosing neon is that a rather substantial amount of effort has already been devoted to the study of its correlation energy by a number of CI calculations.[8-12] These calculations have utilized two different approaches to the CI procedure. The first of these is the Bethe-Goldstone procedure of the type described by Nesbet[8] in which interactions between pairs of spin orbitals are treated by admixing configurations which are not restricted to eigenfunctions of $\vec{L}^2$ and $\vec{S}^2$. The second approach is one developed by Harris and collaborators[10] who have drawn attention to the need for using symmetry-adapted configurations. In this procedure, each nl shell is considered as a whole, and all the excitations from this shell are included in the atomic wave function through the addition of configurations which are eigenfunctions of $\vec{L}^2$ and $\vec{S}^2$. Harris and collaborators have pointed out that such a procedure incorporates interactions between different pairs within each shell, which was neglected in Nesbet's procedure. This pair-pair correlation has also been studied by Barr and Davidson,[11] who have shown that for the $2p$ shell such an effect can be about 15% as important as the total pair-correlation energy between spin orbitals.

The next question of importance is the question of convergence with respect to the angular momentum of the one-electron excited states that are used for the excited configurations in the CI approach. The most extensive CI calculation on neon has been performed by Bunge and Peixoto[12] who have pointed out that excitations to states involving $l=4$ and higher angular momenta contribute about 8% of the correlation energy.

The last point of importance is the question of contributions from configurations involving three-, four-, and more-particle excitations. Estimates of such effects have been made by Barr and Davidson, Bunge and Peixoto, and also by Kestner.[13] These estimates vary between 1 and 5 % of the net correlation energy.

Our LCMBPT calculations to be presented here can also provide answers to these questions by partitioning the diagrams into various classes and also collecting contributions from various l components of $1/r_{12}$. Micha[14] has recently made a diagrammatic study of the importance of pair-pair correlations and excitations involving more than two particles, for the $2p$ shell, using a hydrogenic-type basis set. The relation between this work and ours will be pointed out in Sec. III.

Section II contains a brief review of the LCMBPT procedure as applied to the neon atom. In Sec. III, we present our numerical results on the correlation energy of neon; we also make a comparison of our results and conclusions with those from CI calculations.

II. DESCRIPTION OF PROCEDURE OF CALCULATION AND DIAGRAMS

Since the details of the LCMBPT procedure are available elsewhere,[15-17] we shall give here only the barest essentials for the sake of completeness. The total nonrelativistic Hamiltonian $\mathcal{H}$ for a system of N fermions in interaction via a two-body Coulomb potential is given by (a.u.)[18]

$$\mathcal{H}=\sum_{i=1}^{N} T_i+\sum_{i>j} v_{ij}\ , \tag{1}$$

where T_i is the sum of the kinetic energy and nu-

clear attraction energy operators. The exact ground-state wave function Ψ_0 has to satisfy the eigenvalue equation $\mathcal{H}\Psi_0 = E\Psi_0$, where E is the exact nonrelativistic ground-state energy. In applying perturbation theory, we utilize an approximate Hamiltonian $\mathcal{H}_0$ for which a complete set of basis states can be obtained. Using this basis set, the perturbation is evaluated to various orders in $\mathcal{H}' = \mathcal{H} - \mathcal{H}_0$ through the linked-cluster perturbation approach. For an atom, the most convenient choice of $\mathcal{H}_0$ is the V^{N-1} Hamiltonian,[15] the corresponding lowest eigenstate Φ_0 being the determinant composed of N lowest solutions φ_i having eigenvalues ϵ_i of the equation

$$(T+V)\,\varphi_i = \epsilon_i\,\varphi_i \ . \tag{2}$$

It has been shown that the actual energy E of the system could be derived from the zeroth-order energy E_0 defined by

$$\mathcal{H}_0\Phi_0 = E_0\Phi_0 \tag{3}$$

through the linked-cluster expansion[2]

$$E = E_0 + \langle \Phi_0 | \mathcal{H}' | \Phi_0 \rangle + \sum_{n=1}^{\infty} \langle \Phi_0 | \mathcal{H}' \left(\frac{1}{E_0 - \mathcal{H}_0}\,\mathcal{H}' \right)^n | \Phi_0 \rangle_L \ , \tag{4}$$

the subscript L indicating that only linked terms should be included in the expansion of E. The corresponding total wave function Ψ_0 is given by[2]

$$\Psi_0 = \sum_{n=0}^{\infty} \left(\frac{1}{E_0 - \mathcal{H}_0}\,\mathcal{H}' \right)_L^n \Phi_0 \ . \tag{5}$$

The correlation energy $\Delta E_{\rm corr}$ of the atom is related to E through the equation

$$\Delta E_{\rm corr} = E - E_{\rm HF} \ , \tag{6}$$

where $E_{\rm HF}$ is the Hartree-Fock energy.

The V^{N-1} potential utilized in the present calculation can be described as follows. For the s-basis states, the potential used involved omitting the Coulomb and exchange contribution from one of the $2s$ electrons. The one-electron equations for the s wave functions is then given by

$$\left(\frac{d^2}{dr^2} + \frac{2N}{r} - \frac{1}{r}\left[4\,Y_0(1s^0,\,1s^0;r) + 2Y_0(2s^0,2s^0;r) + 12\,Y_0(2p^0,\,2p^0;r) \right] + 2\epsilon_{ns} \right) P(ns;r)$$
$$+ \frac{2}{r}\left[P(1s^0;r)\,Y_0(1s^0,\,ns;r) + P(2p^0;r)\,Y_1(2p^0,\,ns;r) \right] = 0 \ . \tag{7}$$

The $2s$ wave function from these equations is exactly identical to the HF $2s$ wave function[19] from the V^N potential. The wave function for the $1s$ state, however, is a little different, because the potential used for it does not correspond to the true HF potential. For the non-s states, the potential used involved omitting the spherically averaged Coulomb and exchange potentials due to one of the $2p$ electrons, the corresponding differential equations for the non-s wave functions being

$$\left[\frac{d^2}{dr^2} + \frac{2N}{r} - \frac{l(l+1)}{r^2} - \frac{1}{r}\left(4\,Y_0(1s^0,\,1s^0;r) + 4\,Y_0(2s^0,\,2s^0;r) + 10\,Y_0(2p^0,\,2p^0;r) - \frac{4}{5(2l-1)(2l+3)}Y_2(2p^0,2p^0;r) \right) \right.$$
$$\left. + 2\epsilon_{nl} \right] P(nl;r) + \frac{1}{(2l+1)\,r}\left(2\,P(1s^0;r)\,Y_l(1s^0,\,nl;r) + 2\,P(2s^0,\,r)\,Y_l(2s^0,\,nl;r) \right.$$
$$\left. + \frac{8l(l-1)}{(2l-1)^2}\,P(2p^0;r)\,Y_{l-1}(2p^0,nl;r) + \frac{8(l+1)\,(l+2)}{(2l+3)^2}\,P(2p^0;r)\,Y_{l+1}(2p^0,\,nl;r) \right) = 0 \ , \tag{8}$$

where

$$Y_k(nl,\,n'l';r) = r\int_0^\infty (r_<^k/r_>^{k+1})\,P(nl;r')\,P(n'l';r^1)\,dr' \ .$$

The diagrams originating from the various terms in Eq. (4) will now be discussed. The process of construction of these energy diagrams is greatly facilitated by first considering the wave-function diagrams given by the various terms in Eq. (5). The first-order corrections to Φ_0 are given by the diagrams in Fig. 1. Diagram 1(a) represents the correction to Φ_0 due to the effect of the V^{N-1} potential. Diagrams 1(b) and 1(c) represent the influence of single-particle interactions among the hole (occupied) states and diagram 1(d) represents a true two-body correlation correction. Higher-order corrections to Φ_0 are obtained from these diagrams by inserting additional interaction vertices at the appropriate places. Once the wave-function diagrams are known, the requisite energy diagrams are obtained by terminating the outgoing lines from the wave-function diagrams with appropriate vertices, as required in Eq. (4).

The first term in Eq. (4) is simply the sum of the single-particle energies obtained in our V^{N-1}

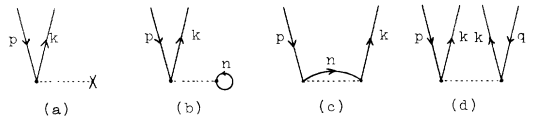

FIG. 1. First-order wave-function diagrams.

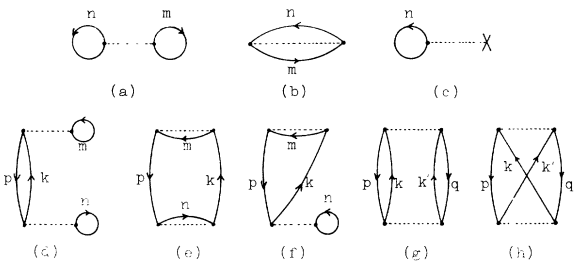

FIG. 2. First- and second-order energy diagrams.

potential. The second term represents the first-order correction to E_0, and when added to E_0 gives the exact HF energy if the one-electron states are generated in the HF potential. However, owing to the use of the V^{N-1} potential in this calculation and the consequent small but finite differences between the energy and wave function for the calculated $1s$ state and those for the HF $1s$ state, we obtain an energy which is not exactly the HF energy, but very close to it. The difference is incorporated by some of the higher-order diagrams to be described below.

The first- and second-order energy corrections to E_0 as given by Eq. (4) are shown in Fig. 2. Diagrams 2(a)–2(c) are the first-order corrections to E_0. Diagrams 2(d)–2(f) and their counterparts with one or both vertices replaced by the V^{N-1} interaction represents single-particle excitation contributions to the energy that arise due to our choice of the single-particle potential, and which shift the one-electron energy towards the true HF energy. With our choice of V^{N-1} potential, diagrams 2(d)–2(f) involve only $1s$ states as hole states. Diagrams 2(g) and its exchange counterpart 2(h) describe the lowest-order pair-correlation energy between the pair p and q.

Algebraic expressions can be written down for the various diagrams through rules given elsewhere.[16,20] These rules will not be repeated here, but instead we shall quote the expressions for typical diagrams in Figs. 2(g) and 2(h) which describe the mutual polarization for electrons in the states p and q:

$$E_2^0(p,q)=\sum_{k,k'}\left(\frac{\langle pq|1/r_{12}|kk'\rangle\langle kk'|1/r_{12}|pq\rangle}{\epsilon_p+\epsilon_q-\epsilon_k-\epsilon_{k'}}-\frac{\langle pq|1/r_{12}|kk'\rangle\langle kk'|1/r_{12}|qp\rangle}{\epsilon_p+\epsilon_q-\epsilon_k-\epsilon_{k'}}\right), \quad (9)$$

the first term arising from the diagram 2(g) and the second term from the diagram 2(h). It is understood that in Eq. (9) sums are taken over all excited states, including continuum, summation being replaced by an integral in the latter case together with an appropriate density-of-states factor. It should be remarked again that whenever p or q represents a $1s$ state, some corrections have to be applied owing to our choice of potential, these corrections being obtained by adding the necessary interaction vertices to the hole line of the type indicated in Figs. 2(d)–2(f).

Figure 3 gives the third-order energy diagrams, with Fig. 3(a) representing hole-hole interactions and Figs. 3(b) and 3(c) corresponding hole-particle interactions. The diagrams 3(b) and 3(c) represent the influence of the interactions of particles in excited states k and k' with the passive unexcited states and with the potential V^{N-1}. The influence of particle-particle interaction (ladder) is shown in Fig. 3(d) which describes the effect of the scattering between particle states on the pair-correlation diagram 2(g). The hole-hole EPV (exclusion principle violating) diagram in Fig. 3(a) and its higher-order ladder counterparts can be shown to form a geometric series, leading effectively to a change in the energy denominator[16] in Fig. 2(g), namely,

$$D(\epsilon_k,\epsilon_{k'})=\epsilon_p+\epsilon_q-\epsilon_k-\epsilon_{k'}+\langle pq|1/r_{12}|pq\rangle-\langle pq|1/r_{12}|qp\rangle\ .$$

Equation (9) is thus modified to

$$E_{2m}(p,q)=\sum_{k,k'}\frac{\langle pq|1/r_{12}|kk'\rangle\langle kk'|1/r_{12}|pq\rangle-\langle pq|1/r_{12}|kk'\rangle\langle kk'|1/r_{12}|qp\rangle}{D(\epsilon_k,\epsilon_{k'})}\ .$$

The summations of hole-particle and particle-particle diagrams in Figs. 3(b)–3(d) to all orders are more involved since they cannot be shown analytically to form exact geometric series. However, an examination of the numerical contributions from successive orders of such interactions indicates that a geometric series is a fairly good approximation. To evaluate the contributions of diagrams 3(b)–3(d), we use the standard definitions[15–17] in the literature for the ratios

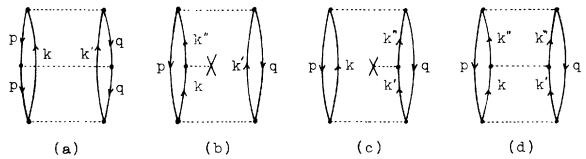

FIG. 3. Third-order energy diagrams involving only one electron pair pq.

$$a(p, q) = E_{3m}^{h\text{-}p}(p, q)/E_{2m}(p, q) , \tag{12}$$

$$t(p, q) = E_{3m}^{p\text{-}p}(p, q)/E_{2m}(p, q) , \tag{13}$$

where $E_{3m}^{h\text{-}p}$ is the contribution from the sum of diagrams in Figs. 3(b) and 3(c) with the modified energy denominator given in Eq. (10). $E_{3m}^{p\text{-}p}$ refers to a similar contribution from the diagram in Fig. 3(d). The contribution to the pair-correlation energy from the pair pq as given by diagrams 2(g) and 2(h) is then modified by the hole-hole, hole-particle, and particle-particle ladder to yield

$$E_2^m(p, q) = E_{2m}(p, q)/(1 - a(p, q) - t(p, q)) . \tag{14}$$

The third-order diagrams in Fig. 3 involve the influence of ladders on the second-order correlation-energy diagrams in Figs. 2(g) and 2(h). These ladder diagrams involve essentially multiple scattering between two electrons in two specific-hole states p and q. However, we can have an analogous set of third-order diagrams which are similar in structure to the ladder diagrams in Fig. 3, but which involve different states on either side of the interaction line representing the ladder. Such diagrams will be referred to as nondiagonal third-order diagrams. Typical diagrams of this class are shown in Fig. 4. Figures 4(a), and 4(b) and 4(c) are hole-hole and hole-particle diagrams while Fig. 4(d) represents a ring diagram which is known to make significant contributions to the correlation energy of an electron gas. There are a number of exchange counterparts of these diagrams and these have been included in our calculations. In earlier investigations on atomic-correlation energies using LCMBPT procedure diagrams of the type shown in Fig. 4 were assumed to be small and were neglected. However, in view of the fact (which will become clear when we present the results in Sec. III) that the diagram 2(g) involving correlation between $2s$ and $2p$ hole states and two different $2p$ hole states makes very important contribution to the correlation energy, it is important to examine quantitatively its third-order partner which is represented by diagrams in Fig. 4, before arriving at any definitive conclusions as to the importance of the latter. As a matter of fact, these are the diagrams which contribute to the pair-pair interactions[11] in CI calculations. This point will be discussed further in Sec. III.

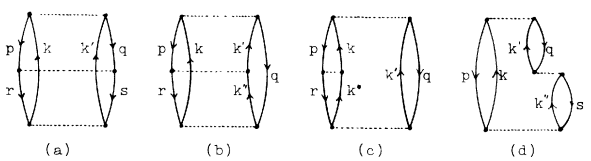

FIG. 4. Third-order nondiagonal energy diagrams involving more than one electron pair.

Figure 5 represent some important fourth-order diagrams. Figures 5(a)–5(b) are typical rearrangement diagrams, and it has been shown earlier in the literature[16] that the effect of such diagrams can also be taken into account to infinite order by shifting the energy denominator. Thus, we modify $D(\epsilon_k, \epsilon_{k'})$ in Eq. (10) to

$$D'(\epsilon_k, \epsilon_{k'}) = D(\epsilon_k, \epsilon_{k'}) + E_2^0(p, q) , \tag{10'}$$

$$D''(\epsilon_k, \epsilon_{k'}) = D'(\epsilon_k, \epsilon_{k'}) + \sum_{r\neq p} E_2^0(q, r) + \sum_{s\neq q} E_2^0(p, s) . \tag{10''}$$

$D'(\epsilon_k, \epsilon_{k'})$ was used to evaluate the correlation energy between a particular pair of spin orbitals p and q, whereas using $D''(\epsilon_k, \epsilon_{k'})$ leads to a correction to the correlation energy between p and q due to three- and more-particle effects. Figure 5(c) is in many respects similar to Figs. 5(a) and 5(b) in that it also represents the effect of three particles being excited at the same time. This effect is included to study the relative importance of three-particle diagrams involving simultaneous three-particle excitations as compared to those involving three particles excited at different times in Fig. 4(d). Figures 5(d)–5(f) are higher-order counterparts of diagram 4(d) involving one more order. The effects of these diagrams and their higher-order counterparts were included by an approximate geometric series procedure through an

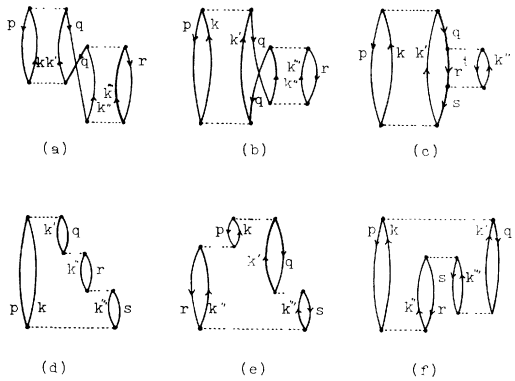

FIG. 5. Typical fourth-order three - and four-body diagrams.

examination of the ratios of contributions from diagrams 5(d)–5(f) with respect to diagram 4(d). These diagrams allow a comparison of contributions from simultaneous four-particle excitations with those from four-particle excitated at different times. Comments about the importance of such multiparticle contributions will be made in Sec. III.

III. RESULTS AND DISCUSSION

There are two aspects to the results we have obtained from the various diagrams discussed in Sec. II. First, we would like to present quantitative results for such physical effects as pair correlation, pair-pair correlation, and other effects outlined in the Introduction. A comparison of these results will then be made with corresponding results obtained by CI calculations. The second aspect of our results is the total correlation energy, its comparison with experiment and with previous calculations. For the first, we require combinations of contributions from various classes of diagrams that are pertinent to the physical effects of interest. The comparison of our results and conclusions with those from CI calculations will be greatly facilitated by first summarizing the results that have been obtained from the latter.

A. Review of CI Calculations

A summary of the main results obtained by various CI calculations is presented in Table I, together with results of similar type that we have obtained from our diagrams. The second column lists the maximum value of l that was used for the excited states in the CI calculations. The third column gives the net correlation energy obtained from excitations of a pair of orbitals at a time without requiring the net excited wave function to be an eigenfunction of $\vec{L}^2$ and $\vec{S}^2$. Such a correlation mechanism will be referred to as pair correlation between spin orbitals. The next column gives symmetry-adapted pair correlation energies where pair excitations are considered from one or two nl shells at a time, taking care to make the wave function for the excited state an eigenfunction of $\vec{L}^2$ and $\vec{S}^2$. The next column which is called the full CI up to pairs describes the results obtained when all the symmetry-adapted pair excitations are considered together. These last two procedures allow for what are called pair-pair correlation interactions. The first of these incorporates diagonal pair-pair correlation such as, for example, the interaction between two $2s$-$2p$ excitations or two $2p$-$2p$ pair excitations. The second full CI calculation includes also the nondiagonal pair-pair correlation effect, such as the interaction between $2s$-$2p$ and $2p$-$2p$ pairs. The last column represents contributions from triple and quadruple excitations. Triple and quadruple excitations are defined in this context as involving excited configurations in which three and four particles are excited simultaneously.

A comparison of the results in one column or between results in various columns then allows conclusions to be drawn regarding the dependence of the correlation energy on l, the importance of pair-pair correlations with respect to pair correlations, and finally, multiple excitations compared with pair excitations. Additionally, a comparison of results in any one column, for the same value of l, by two different groups of investigators, leads to information on the dependence of the calculated correlation energies on the choices made for the radial functions for the one-electron orbitals.

Nesbet's earliest calculation[8] refers to spin-orbital correlations. As may be seen from Table I, he obtained a very good answer for the correlation energy, namely, 98% of experiment, by going only up to $l=3$. Nesbet, Barr, and Davidson's (NBD)[9] later spin-orbital correlation result including excited states up to $l=6$ exceeds Nesbet's correlation energy by about 7.5% (of the experimental correla-

TABLE I. Summary of various CI calculations and results from present calculations (in a.u.).

Reference	Max l	Spin-orbital pair sum	Symmetry-adapted pair	Full CI up to pairs	Triple and quadruple
Nesbet (Ref. 8)	3	−0.382 227			
NBD (Ref. 9)	6	−0.410 300			
VHS (Ref. 10)	3	−0.373 774	−0.335 55	−0.329 216	
BD (Ref. 11)	3	−0.395 88		−0.333	−0.005 74[a]
BP[a] (Ref. 12)	3			−0.350	−0.004
	$l>3$			−0.385	
Present calculation	3	−0.394 89	−0.367 58	−0.372 45	0.003
	6	−0.413 26	−0.385 95	−0.390 82	

[a]The second line includes estimated contributions from all values of l.

tion energy), leading to a larger correlation energy than experiment. It would have been interesting to compare NBD's spin-orbital correlation energies with those from symmetry-adapted pair correlation and full CI calculations with the same choice of basis functions, but no such results have been reported by NBD. The next set of results in Table I is that due to Viers, Harris, and Schaefer (VHS)[10] which is the first calculation beyond Nesbet's that included pair-pair correlation within the CI framework. VHS's results in the first column of Table I refers to spin-orbital correlation and should be comparable with Nesbet's earlier work, because they used the same upper limit on l (up to 3) for excited states. However, there appears to be a difference of about 2.5% between the two results, which is an indication of the effect of using two different radial basis sets. The result of VHS in the second column indicates that when they used symmetry-adapted pairs, the diagonal pair-pair interactions led to a decrease in the correlation energy by about 10%. Finally, when they utilized the full CI procedure, there was a smaller but finite additional decrease (1.5%) in the correlation energy due to nondiagonal pair-pair interactions. Their results thus indicate that both diagonal and nondiagonal pair-pair interactions lead to contributions to the correlation energy of opposite sign than that from pair correlation effects. The next row in Table I refers to the results of Barr and Davidson (BD).[11] These authors do not give results for symmetry-adapted pair-correlation energies for various shells. Instead they have presented their results from spin-orbital pair correlations and from full CI calculations. In agreement with the trend observed by VHS, the pair-pair correlation energy (of about 15% of net correlation energy) has opposite sign to the pair-correlation energy. There is again a small difference between the spin-orbital pair-correlation-energy results of VHS and BD due to the different radial basis sets chosen. BD also performed a perturbation calculation to estimate the contribution from triple and quadruple excitations, and obtained about 1.5% of the net correlation energy with the same sign as for pair-correlation energy. The next row lists the results of the most extensive CI calculation of Bunge and Peixoto (BP).[12] Unfortunately, BP did not present numbers that strictly belong to the second and third columns, but they do have two results for the fourth column: one for $l \leq 3$, while the other is stated to include contributions from all l. These results indicate that when g, h, and higher harmonics are included, the correlation energy is increased[21] by about 8%, bringing the theoretical results into very close agreement with experiment. They also studied the importance of triple and quadruple excitations, and arrived at the conclusion that about 1% of the net correlation energy originated from these many particle excitations. It should also be noted that there is a small but significant difference (5%) between the full CI results of BP for $l \leq 3$ and the corresponding results of VHS and BD. This difference is perhaps again the result of different radial basis sets used in the three cases, BP's choice being more flexible.

Summarizing, we arrive at the following conclusions regarding CI results. First, convergence in l seems to be rather important and accounts for about 8% of the net correlation energy. Second, pair-pair correlation effects are important mainly for the L shell and account for a decrease in the correlation energy by about 10–15%. In the pair-pair correlation mechanisms, nondiagonal effects are seen from the VHS calculation to be an order of magnitude weaker than the diagonal effects and account for only 1.5% of the correlation energy. As indicated at various points in comparing different calculations using the same value of l, there seems to be a small but finite dependence of the calculated correlation energy on the radial basis sets that have been used in the various CI calculations. Finally, the full CI calculation by BP with substantial flexibility in the radial basis functions and in angular excitations (l), does lead to very good agreement with the experimental correlation energy.

B. One-Electron Energy by LCMBPT Procedure—Comparison with HF Energy

The contributions from the various LCMBPT diagrams will now be presented and analysed. The emphasis in the discussion that follows will be both on obtaining detailed understanding of various types of correlation effects that occur in neon and also on studying whether conclusions from LCMBPT procedure agree with those just listed from an analysis of various CI calculations.

In Table II, the numerical results for the one-particle contributions to the energy of the neon atom are presented. The numbers in the first three rows are the eigenvalues of $1s$, $2s$, and $2p$ states in the V^{N-1} potential. Since Clementi's HF wave functions were used to generate the V^{N-1} potential from which the basis set of states was calculated, the close agreement for $2s$ and $2p$ between the eigenvalues that we have obtained and Clementi's values is a good indication of the numerical accuracy of our procedure for basis-set calculation. The sizable difference between our $1s$ eigenvalue and that of Clementi was anticipated from our choice of V^{N-1} potential, described in Sec. II. The effect of this departure from the HF $1s$ energy on diagrams involving $1s$ states is incorporated through the laddering procedure which has been discussed earlier in the literature and will be utilized in this

TABLE II. Single-particle contributions to the energy (in a.u.).

Diagram	Description	Contribution[a]	
	$2\epsilon_{1s}$	−68.25404	(−65.54552)
	$2\epsilon_{2s}$	−3.86116	(−3.86096)
	$6\epsilon_{2p}$	−5.10318	(−5.10288)
Subtotal	E_0	−77.21838	
$2(a)+2(b)$	$n=1s;\ m=1s$	−25.59923	
$+2(c)$	$n=1s;\ m=2s$	5.61959	
	$n=1s;\ m=2p$	16.71489	
	$n=2s;\ m=2s$	−17.33898	
	$n=2s;\ m=2p$	10.69924	
	$n=2p;\ m=2p$	−41.42542	
Subtotal	$\langle\Phi_0\lvert\mathcal{H}'\rvert\Phi_0\rangle$	−51.32991	
Total		−128.54829	(−128.54701)
$2(d)+2(e)$ $+2(f)$	Single-particle excitation	−0.00003	
Grand total		−128.54832	

[a]Numbers in parenthesis are from Clementi's calculation (Ref. 19).

work. The 5th–10th rows of Table II show the contributions from the first-order diagrams 2(a)–2(c). The sum of the single-particle energies E_0 and the first-order correction to the energy adds up to −128.54829 a.u., which is very close to Clementi's HF value (−128.54701 a.u.). It is interesting to note that while the sum of the one-electron energies for V^{N-1} potential differs from the corresponding HF value by 2.70902 a.u., the first-order corrections given by Figs. 2(a)–2(c) neutralize[15] most of this difference, bringing the final total energy up to the first order, in close agreement with the corresponding HF value.

C. Pair-Correlation Energy—Comparison with CI Results

Figures 2(g) and 2(h) represent the pair-correlation contributions to the energy. The algebraic expression for the contributions to the energy from these diagrams is given in Eq. (9).

In our calculations, we have included all bound states to $n=10$ for each value of the angular momentum quantum number. For continuum states we employed 12 Gauss-Laguerre points with $k_{\max}=15\,a_0^{-1}$. The most important contribution to the correlation energy from the continuum states came from $k=0\sim 2a_0^{-1}$. The continuum states were found to contribute about 90% of the pair-correlation energy. This is not unexpected, because of the following reasons. The closest bound excited state to $2s$ and $2p$ is the $3s$ state, and the energy differences for excitation involving this excited state are not very different from those for low-k states with energy differences comparable to ionization energy. However, the matrix elements that occur in the numerators of Eq. (9) are much larger for the continuum states because of greater overlap with $2s$ and $2p$ states than is the case for the bound excited states. A combination of these two factors explains the preponderance of the contributions from the continuum states.

In Table III, a detailed breakdown of contributions to the pair-correlation energy among the states of the $2p$ shell, from excited states corresponding to various l values, are presented. The major contributions to the pair-correlation energy arise from $2p^2\rightarrow kpk'p$ and $2p^2\rightarrow kdk'd$ excitations corresponding, respectively, to the monopole and dipole components of $1/r_{12}$. The radial matrix elements that occur in the evaluations of diagrams for these excitations are comparable in order of magnitude for the monopole and dipole cases, the actual magnitude being about a factor of 4 or 5 larger for the latter case as compared with the former. However, the net contribution to the pair-correlation energy from the two types of excitations is comparable in magnitude because of the larger angular factors that oc-

TABLE III. Contributions to the $2p$-$2p$ pair-correlation energies from diagrams 2(g) and 2(h) (in a.u.).

Excitations	Direct	Exchange	Total
(s,s)	−0.00891	0.00594	−0.00297
(p,p)	−0.14384	0.01970	−0.12414
(d,d)	−0.11556	0.01425	−0.10131
(f,f)	−0.01755	0.00302	−0.01453
(g,g)	−0.00476	0.00145	−0.00331
(h,h)	−0.00176	0.00060	−0.00116
(i,i)	−0.00059	0.00011	−0.00048
(s,d)	−0.01532	0.00761	−0.00762
(p,f)	−0.00628	0.00193	−0.00435
(d,g)	−0.00568	0.00168	−0.00400
(f,h)	−0.00201	0.00062	−0.00139
(g,i)	−0.00071	0.00015	−0.00056
Total	−0.32288	0.05706	−0.26582

TABLE IV. Modified $2p$-$2p$ pair-correlation energies in a.u.

Excitations	$E_{2m}(2p,2p)$ Direct	Exchange	Total	$E_2^m(2p,2p)$ Total
(s,s)	−0.00760	0.00507	−0.00253	−0.00286
(p,p)	−0.12258	0.01711	−0.10547	−0.11527
(d,d)	−0.10572	0.01302	−0.09270	−0.09707
(f,f)	−0.01585	0.00281	−0.01304	−0.01398
(g,g)	−0.00425	0.00128	−0.00297	−0.00313
(h,h)	−0.00160	0.00056	−0.00104	−0.00107
(i,i)	−0.00053	0.00010	−0.00043	−0.00044
(s,d)	−0.01374	0.00690	−0.00684	−0.00721
(p,f)	−0.00565	0.00175	−0.00390	−0.00424
(d,g)	−0.00507	0.00147	−0.00360	−0.00372
(f,h)	−0.00180	0.00055	−0.00125	−0.00130
(g,i)	−0.00063	0.00013	−0.00050	−0.00053
Total	−0.28502	0.05075	−0.23427	−0.25082

TABLE V. $2s$-$2p$ pair-correlation energies in a.u.

Excitations	E_{2m} Direct	Exchange	Total	E_2^m Total
(s,p)	−0.066 76	0.020 20	−0.046 56	−0.049 68
(p,d)	−0.030 00	0.011 76	−0.018 24	−0.018 56
(d,f)	−0.022 64	0.004 62	−0.018 02	−0.019 27
(f,g)	−0.007 13	0.002 44	−0.004 69	−0.004 93
(g,h)	−0.003 07	0.001 40	−0.001 67	−0.001 75
(h,i)	−0.000 98	0.000 29	−0.000 69	−0.000 72
Total	−0.130 58	0.040 71	−0.089 87	−0.094 91

cur in the monopole case. The net $2p$-$2p$ pair contribution from diagrams 2(g) and 2(h) is seen to be −0.265 82 a.u., which is composed of the direct contribution −0.322 88 a.u. and the exchange contribution +0.057 06 a.u.

We next discuss the question of ladder[16] corrections to these pair-correlation energy diagrams. Inclusions of hole-hole interactions in Fig. 3(a) and rearrangement corrections in Figs. 5(a) and 5(b) up to all orders give the modified correlation energy $E_{2m}(p, q)$ as in Eq. (11), with the denominator $D(\epsilon_k, \epsilon_{k'})$ being replaced by $D'(\epsilon_k, \epsilon_{k'})$ in Eq. (10′). These modified correlation energies $E_{2m}(p, q)$ are listed in the second, third, and fourth columns of Table IV. These corrections were found to be quite important and amounted to about a 12% decrease of $E_2^0(p, q)$ as given in Table III. The hole-particle and particle-particle interactions shown in diagrams 3(b)–3(d) were included using Eq. (14), with the appropriate ratios a and t given in Eqs. (12) and (13). Typically, we found $a(2p, 2p) = -0.20$ and $t(2p, 2p) = 0.29$ for monopole excitations. This leads to the net $2p$-$2p$ pair-correlation energy $E_2^m(2p, 2p)$, which is shown in the last column of Table IV. As can be seen from this Table, inclusion of hole-particle and particle-particle ladders cancels out more than 50% of the contributions from the hole-hole and rearrangement corrections terms.

It should be remarked that we have used only the monopole component of $\mathcal{H}'$ interaction in the ladders. Use of higher-multipole component of $\mathcal{H}'$ would require at least two interaction vertices at a time to conserve the angular momentum. Thus, the first finite correction will come from diagrams which are two orders higher than the parent diagram. Corrections due to these effects are expected to be much smaller than the monopole interactions and were neglected. A conservative error estimate of this approximation is only 0.002 a.u.

TABLE VI. $2s$-$2s$ pair-correlation energies in a.u.

Excitations	E_{2m}	E_2^m
(s,s)	−0.003 30	−0.003 54
(p,p)	−0.001 89	−0.001 93
(d,d)	−0.004 85	−0.005 09
(f,f)	−0.001 26	−0.001 34
(g,g)	−0.000 46	−0.000 49
(h,h)	−0.000 19	−0.000 20
(i,i)	−0.000 09	−0.000 09
Total	−0.012 04	−0.012 68

TABLE VII. Pair-correlation energies involving $1s$ states (in a.u.).

Pair	Excitation	Direct	Exchange	Total
$1s$-$2p$	(s,p)	−0.004 54	−0.001 93	−0.006 47
	(p,d)	−0.015 89	0.003 39	−0.012 50
	(d,f)	−0.006 09	0.001 52	−0.004 57
Total		−0.026 52	0.002 98	−0.023 54
$1s$-$2s$	(s,s)	−0.002 58	0.001 25	−0.001 33
	(p,p)	−0.002 84	0.000 62	−0.002 22
	(d,d)	−0.000 61	0.000 18	−0.000 43
	(f,f)	−0.000 10	0.000 04	−0.000 06
Total		−0.006 13	0.002 09	−0.004 04
$1s$-$1s$	(s,s)	−0.009 06		−0.009 06
	(p,p)	−0.016 78		−0.016 78
	(d,d)	−0.001 22		−0.001 22
	(f,f)	−0.000 21		−0.000 21
Total		−0.027 27		−0.027 27

In Tables V and VI, we have presented the pair-correlation contributions from $2s$-$2p$ and $2s$-$2s$ diagrams. The contributions are listed in two stages, namely, after incorporation of hole-hole interactions and rearrangement diagrams, as in Table IV for the $2p$-$2p$ correlation, while the last column presents the numbers, including hole-particle and particle-particle ladders as well. The net correlation energy from the $2s$-$2p$ diagrams, modified by its ladders, is thus a little more than one-third of the $2p$-$2p$ correlation energy. The $2s$-$2s$ correlation energy, on the other hand, is an order of magnitude smaller and only about 5% of the $2p$-$2p$ correlation energy.

For correlations involving $1s$ states, namely, $1s$-$2p$, $1s$-$2s$, and $1s$-$1s$ interactions, the net contributions are listed in Table VII. In this case we have listed only the net contributions to the direct and exchange diagrams after incorporating all the ladder corrections, namely, hole-hole interaction, rearrangement diagrams, hole-particle, and particle-particle interactions. The convergence with respect to l for correlations involving the $1s$ state was very rapid, and it was found sufficient to include particle states with $l \leq 3$. The major correlation effect involving the $1s$ states arises from the $1s$-$1s$ and $1s$-$2p$ interactions. While the net contribution from the $1s$-$2p$ correlation including all

TABLE VIII. Comparison of pair-correlation energies from LCMBPT procedure with those of CI calculations (in a.u.).

	This work		Nesbet (Ref. 8)	NBD (Ref. 9)	VHS (Ref. 10)	BD (Ref. 11)
Max pairs	3	6	3	6	3	3
$2p$-$2p$	−0.240 63	−0.250 82	−0.224 89	−0.243 07	−0.216 46	−0.233 45
$2p$-$2s$	−0.087 51	−0.094 91	−0.081 55	−0.090 55	−0.082 65	−0.084 78
$2s$-$2s$	−0.011 90	−0.012 68	−0.010 83	−0.011 73	−0.011 33	−0.011 17
L-shell total	−0.340 04	−0.358 41	−0.317 27	−0.345 35	−0.310 44	−0.329 40
$2p$-$1s$	−0.023 54		−0.019 89		−0.019 35	−0.021 27
$2s$-$1s$	−0.004 04		−0.005 14		−0.005 02	−0.005 28
$1s$-$1s$	−0.027 27		−0.039 93		−0.038 97	−0.039 93
Total	−0.394 89	−0.413 26	−0.382 23	−0.410 31	−0.373 78	−0.395 88

$2p$ states is comparable to the $1s$-$1s$ contribution, the $1s$-$2p$ correlation energy per $2p$ state is a factor of 7 smaller than the $1s$-$1s$ interaction. This is expected because $1s$-states overlap much more strongly with each other than with $2s$ or $2p$ states. The net contributions to the correlation energy from interactions involving $1s$ states is found to be −0.054 85 a.u. and is about 20% of the $2p$-$2p$ correlation energy. Combining all the pair correlation contributions from Tables IV–VII, we find a total of −0.413 26 a.u.

Table VIII presents a comparison of various individual pair-correlation contributions to the energy obtained by us with those from CI calculations. A comparison is also made of the net L-shell pair-correlation energies. The main features of the relation between our results and the CI results are the following. For L-shell correlation energies, there is a substantial increase in going from $l \leq 3$ to $l \leq 6$ (about 5%). A similar observation can be made for the CI calculations, namely, in going from Nesbet's results to those of NBD where an increase of about 8% is observed. The second feature is that the difference between our L-shell correlation energy and that obtained by CI calculations is actually somewhat smaller than the variation among the various CI calculations. This feature is again an indication of the sensitiveness of variational calculations to the choice of radial basis functions, which makes their exact comparison with perturbation calculations a little ambiguous. The third feature is the $1s$-$1s$ correlation energy. Our $1s$-$1s$ pair-correlation energy is about 0.012 a.u. lower than that from CI calculations. While this difference is within the error limit of our calculation, it is still significant, and deserves some comment. We feel that the origin of this difference can be traced to our use of the V^{N-1} potential which makes the $1s$ energy and wave function somewhat different from those for the HF (V^N) case. The effects of the difference in single-particle energy on the individual diagrams, as pointed out earlier, are corrected by various ladder diagrams. However, the difference in the wave functions could still influence the values of individual diagrams. We feel that this difference is distributed among other pair-correlation energies, with the sum of all the pair-correlation energies being comparable in the two cases, where one starts with the V^N or V^{N-1} potentials.

D. Pair-Pair Correlation Contribution to the Energy

The diagrams 4(a)–4(d) are the nondiagonal third-order energy diagrams discussed in Sec. II. Their diagonal counterparts have already been incorporated as ladders to pair-correlation diagrams. These nondiagonal third-order diagrams represent pair-pair correlations because they consist of interactions between initial and final states involving different pairs excited from the vacuum. Some of these pair-pair correlation effects are incorporated in the symmetry-adapted pair CI calculation, while some others require a full CI calculation. In Table IX, the numerical contributions from the diagrams 4(a)–4(d) are summarized. Unfortunately, the series associated with various higher-order counterparts of these diagrams cannot be summed exactly as geometric series. However, since the diagram 4(d) gives the major contribution, we felt it necessary to incorporate its higher-order effects represented by diagrams 5(d) and 5(e) and associated higher-order diagrams, assuming the geometric series behavior to hold approximately. For this purpose, the geometric-series ratio was obtained by comparing the contributions of diagrams 5(d) and 5(e) to the diagram 4(d). The higher-order counterparts of Figs. 4(a)–4(c) are expected to be small and the neglect of these diagrams should not give rise to an error

TABLE IX. Contributions from the nondiagonal third-order energy diagrams (a.u.).

Diagrams	Descriptions	Contributions
4(a)	$(p,q;r,s)$	
	$=(2p,2p;2p,2p)$	$-0.000\,27$[a]
	$=(2s,2p;2p,2s)$	$0.000\,56$[b]
	$=(2s,2s;2p;2p)$	$0.001\,65$[c]
4(b)	$(p,q;r)$	
	$=(2p,2p;2p)$	$-0.000\,03$[a]
	$=(2p,2s;2p)$	$-0.000\,31$[b]
	$=(2s,2p;2p)$	$-0.001\,69$[d]
	$=(2s,2s;2p)$	$-0.000\,92$[e]
4(c)	$(p,q;r)$	
	$=(2p,2p;2p)$	$-0.004\,03$[a]
	$=(2p,2s;2p)$	$-0.002\,14$[b]
	$=(2p,2p;2s)$	$-0.008\,38$[d]
	$=(2p,2s;2s)$	$-0.002\,64$[e]
4(d)	$(p,q;s)$	
	$=(2p,2p;2p)$	$0.025\,42$[a]
	$=(2p,2s;2s)$	$0.002\,05$[b]
	$=(2s,2p;2p)$	$0.006\,06$[b]
	$=(2p,2p;2s)$	$0.004\,85$[d]
	$=(2s,2p;2s)$	$0.002\,26$[e]
Total		0.022 44

[a]Diagonal pair-pair interaction between two $2p$-$2p$ pairs.
[b]Diagonal pair-pair interaction between two $2s$-$2p$ pairs.
[c]Nondiagonal pair-pair interaction between the pairs of $2s$-$2s$ and $2p$-$2p$.
[d]Nondiagonal pair-pair interaction between the pairs of $2s$-$2p$ and $2p$-$2p$.
[e]Nondiagonal pair-pair interaction between the pairs of $2s$-$2s$ and $2s$-$2p$.

greater than 0.0015 a.u. [about 10% of the net contribution from diagrams 4(a)–4(c)]. In addition to presenting the net contributions of these various pair-pair diagrams 4(a)–4(d) in Table IX, we have also broken down the contributions from different pairs of hole states. This allows us to examine contributions from different modes of pair-pair interactions, namely, diagonal ones such as those between two $2p$-$2p$ pair excitations, or two $2s$-$2p$ pair excitations, and nondiagonal ones such as those between the pairs of $2s$-$2s$ and $2p$-$2p$, $2s$-$2s$ and $2s$-$2p$, or $2s$-$2p$ and $2p$-$2p$.

The net contributions from these different modes of pair-pair correlations, obtained by making appropriate summations from Figs. 4(a)–4(d), are listed in Table X. We notice that the major contribution arises from the pair-pair interactions involving $2p$-$2p$ pairs. On adding this contribution to our $2p$ pair-correlation energy ($l \leq 3$), we obtain the net $2p$-$2p$ correlation energy which can be compared with the symmetry-adapted pair-correlation energy involving the $2p$ states. Our value for this energy is $-0.219\,54$ a.u. ($l \leq 3$) as compared with $-0.185\,62$ a.u. from the CI calculations of VHS.[10] The corresponding number we obtained on including excitations up to $l=6$ in the pair correlation energy was $-0.229\,73$ a.u.

Some other theoretical numbers with which our pair-correlation and pair-pair correlation energies can be compared are those from recent calculations by BD[11] and Micha.[14] BD examined only $p \rightarrow p$ excitations, and found that pair-pair interaction amounts to about 15% of the pair-correlation energy. They also found the same ratio between the pair-correlation energy and the correlation energy from the full CI calculations, their results for the two cases being -0.396 and -0.333 a.u., respectively. As far as Micha's perturbation calculation is concerned, it is difficult to make a detailed numerical comparison of individual contributions from our calculations and his because of his choice of a different basis set and the approximations that he used in evaluating the continuum contributions. However, his ratio of the contribution from pair-pair interaction to that from pair correlations for the $2p$ shell is 0.10, which is comparable to our ratio of 0.084 for this case.

We do not have any numbers available from CI calculations to compare with the nondiagonal pair-pair correlation energies listed in Table X. However, their net sum could be compared with the difference between the full CI and symmetry-adapted pair results of VHS. While we find a net negative contribution of $-0.004\,87$ a.u. for this difference, VHS found a net positive contribution of 0.006 34 a.u. It would have been interesting if results were available from the other CI calculation to make a similar comparison. In view of the smallness of this net contribution, however, the difference between our results and those of VHS, as far as the total correlation energy is concerned, is not very serious.

E. Importance of Various Multipole Contributions to the Pair-Correlation Energy

We would like next to remark on the question of convergence in l and its influence on the correlation energy. Already, while discussing the pair-correlation energy, it was remarked that we found

TABLE X. Contributions from diagonal and nondiagonal pair-pair interactions (in a.u.).

Pair-Pair	Contributions
Diagonal	
$(2p2p)$-$(2p2p)$	0.021 09
$(2s2p)$-$(2s2p)$	0.006 22
Nondiagonal	
$(2s2s)$-$(2p2p)$	0.001 65
$(2s2p)$-$(2p2p)$	$-0.005\,22$
$(2s2s)$-$(2p2s)$	$-0.001\,30$
Total	0.022 44

about a 5% increase (with respect to experimental-correlation energy) in the pair-correlation energy in going from $l \leq 3$ up to $l \leq 6$. This result is in reasonable agreement with a similar increase of 8% found by comparing Nesbet's pair-correlation energy[8] with $l \leq 3$ with the NBD result[9] for $l \leq 6$. Bunge and Peixoto[12] have carried out the most detailed CI calculations on neon. Unfortunately, they have not split up their correlation energies into pair and pair-pair contributions. However, their result from the full CI calculation has been split up into two parts, the first being the contribution from $l \leq 3$ configurations and the second from g, h, and higher harmonic excitations. They also found about an 8% increase from l excitations higher than 3. From both CI and our perturbation calculations, it thus appears that the contribution to the correlation energy from $l > 3$ varies from 5 to 8%, and is comparable in importance to the pair-pair correlation energy. It appears then that if one is interested in the kind of accuracy that we are now interested in in terms of comparison with experiment, it is very essential to include both pair-pair correlation energy and l excitations higher than $l = 3$ and at least up to $l = 6$. This variation with range of l combined with the calculated pair-pair contributions, allows us to make estimates of the errors expected in some cases where we neglected contributions from both higher l states beyond $l = 3$ and from pair-pair interactions. This is the case for our calculated correlation energies involving $1s$ states. The contribution to the total pair-correlation energy from pair interactions involving $1s$ states was found to be only $-0.054\,85$ a.u. If we assume the above-mentioned trend that we found in l convergence, then the inclusion of higher l beyond 3 would increase pair-correlation energy by about 5% of $-0.054\,85$ a.u. Also assuming the observed trend in pair-pair interactions found for the L shell, pair-pair interactions involving the $1s$ states would be expected to reduce the pair-correlation energy ($-0.054\,85$ a.u.) by about 6%. The combined effects of the neglect of $l > 3$ and pair-pair interactions are thus seen to mutually cancel, leading to only about a 1% net decrease.

F. Many-Particle (>2) Contributions to the Correlation Energy

We would like to consider next the question of many-particle excitation contribution to the correlation energy of neon. By many-particle contributions, we mean contributions from more than two particles. In diagrammatic language one can try to make some conventions as to what to call three-, four-, and more-particle excitation diagrams as compared to two-particle ones. For example, while the pair-excitation diagrams in Figs. 4(a)–4(d) involve more than two one-electron states,

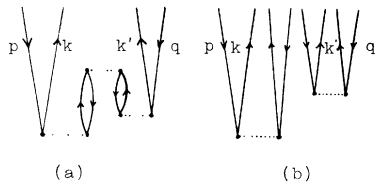

FIG. 6. Some wave-function corrections due to many-particle (>2) excitations.

one cannot call them many-particle excitation diagrams, because at any instant only two-hole states are excited. The same remark applies also to diagrams 5(d) and 5(e). Figure 5(f) represents another interesting example, where some discretion is needed in deciding whether to regard it as a two-particle diagram or not. If one makes a convention that an n-particle diagram will be one in which at any instant there are n particles excited simultaneously, then the diagram 5(f) would be called a four-particle diagram. In the CI calculation, when one talks about pair excitation, what one is really talking about is that in the wave function of the atom there are only two-particle excitations at one time. However, since CI calculations are not carried out perturbationwise but rather using variation procedures, the pair-excitation wave function could involve both diagrams like the ones in Fig. 1(d) as well as diagrams of the type in Fig. 6(a). The latter diagrams get incorporated through interactions between matrix elements between various pair functions in the process of solving the secular equation for the variation procedure. If the CI calculation in fact incorporates the type of (averaged) three- or more-particle excitations represented typically by Fig. 6(a), then some of of the four-particle contribution from Fig. 5(f) could come from the pair-excitation wave function of the CI procedure. However, diagram 5(f) could also be constructed from four-particle functions of the type in Fig. 6(b) and contributions of this type to the correlation energy are referred to as four-particle contributions. Thus, in order to compare the CI results with the correlation energy contribution we have obtained from diagram 5(f) it is necessary to make a separation of the CI contributions to this diagram from pair excitations and four-particle excitations of the CI language. Unfortunately, such a separation has not been provided for available CI calculations.

This situation is reminiscent of a similar situation that occurs in variational unrestricted Hartree-Fock (UHF) and PUHF (projected unrestricted Hartree-Fock) calculations,[22] where in trying to make the one-electron orbitals different from one another because of the different exchange with outer electrons, one introduces an inadvertent

amount of correlation. This can be seen in the case of PUHF calculations, from the fact that a combination of more than one determinant is used and in the case of UHF calculations, through the fact that the difference in the wave functions for different spin states may not just be due to exchange, but also due to the intrashell correlations, which keep the electrons apart from each other.

In our LCMBPT calculation, we regard the contributions from the diagrams of the type in Fig. 5(f) to represent the influence of quadruple excitations on the energy. In view of the above remarks about the nature of many particles in CI procedures, one cannot make an exact quantitative comparison between our many-particle contributions and those from CI calculations. However, the two should be of comparable order of magnitude. We obtained 0.006 03 a.u. from diagrams 5(a) and 5(b) ($p \neq r$) and − 0.003 48 a.u. from the diagram 5(f). The sum of these two numbers is listed under many-particle contribution in Table XI together with various one- and two-particle contributions. Estimates of three- and four-particle excitation contributions made by Barr and Davidson and by Bunge and Peixoto vary from 1–1.5% of net correlation energy and this conclusion is in reasonable order-of-magnitude agreement with ours. There are a number of diagrams with similar topological structure as 5(c) but with different arrangements of interaction lines. We have not included any of these diagrams as well as 5(c) in our many-particle result. Additionally, there are some other diagrams with the same structure as diagrams 5(a) and 5(b) but with different choices and arrangements of hole and particle lines. These diagrams were also neglected. The upper limit of error due to this neglect of some of the higher-order diagrams was estimated to be less than 0.004 a.u. From Table XI, the final result of our calculation of the correlation energy of neon is seen to be − 0.389 14 a.u.

TABLE XI. Summary of contributions to the correlation energy.

Descriptions	Contributions (a.u.)
$E_0 + \langle \Phi_0 \vert \mathcal{H}' \vert \Phi_0 \rangle$	−128.548 29
Single excitation	− 0.000 03
$\sum E_2^{\pi}(p, q)$	− 0.413 26
Third-order nondiagonal	0.022 44
Many-particle excitations	0.002 99
Total	− 128.936 15
E_{HF} (Clementi)	− 128.547 01
ΔE_{corr}	− 0.389 14

G. Comparison of Total Correlation Energy with Experiment and CI Results

In comparing the theoretically calculated energy with experiment, there are two ways that one can proceed. One is to add the relativistic and radiative corrections to the calculated total energy and compare this sum with the sum of the experimental ionization energies for all the electrons. The other procedure is to subtract from the experimental energy relativistic and radiative corrections, and then obtain the experimental nonrelativistic energy. From the experimental energy obtained in this way one can subtract the HF energy and get the nonrelativistic correlation energy which is to be compared with the results of our LCMBPT and the various CI calculations. This latter process of comparison between experiment and theory is the one that has been used in the literature on neon and we would like to summarize briefly the situation regarding the experimental nonrelativistic correlation energy obtained in this manner. The experimental total energy for neon as quoted by Scherr *et al.*[23] is − 129.0601 a.u. For the relativistic correction we have chosen to use the results of Kim's Dirac-Hartree-Fock (DHF) calculations.[24] One can obtain the relativistic correction to the energy by subtracting from Kim's DHF result the nonrelativistic HF energy. By this procedure one gets a relativistic correction of − 0.1330 a.u. This number has to be subtracted from the experimental energy to incorporate the relativistic correction. There is an additional correction to be considered which is connected with the interaction of the electron with its radiation field. This effect arises mainly from the 1*s* electrons and is estimated to be about 0.0086 a.u. by Hartman and Clementi.[25] This number also has to be subtracted from the experimental total energy. Combining the relativistic and radiative corrections, one obtains the net correction of − 0.1244 a.u., which has to be subtracted from the experimental energy. This correction to the energy compares very well with the corresponding value of − 0.1226 a.u. obtained by Hartman and Clementi, the small difference of 0.0018 a.u. owing to the fact that Hartman and Clementi's relativistic correction[25] was obtained using a perturbation approach instead of using the DHF results for the energy which was done here. On combining these effects, one gets the "experimental nonrelativistic energy" of − 128.9357 a.u. which, using HF energy of − 128.5470 a.u., leads to − 0.3890 a.u. ± 0.001 a.u. for the correlation energy of neon. There are some additional corrections to be considered which are expected to be quite small. First, there is the mass polarization effect which is a correction to the electron-electron interaction due to the influence of nuclear motion. The esti-

TABLE XII. Comparison of the total correlation energy with experiment and various CI results.

Authors	ΔE_{corr} (a.u.)
Experiment	-0.3890 ± 0.001
Present calculation	-0.38914 ± 0.01
Nesbet	-0.38223
NBD	-0.4103
VHS	-0.33555
BD	-0.333
BP	-0.385 ± 0.008

mate of this effect on the energy for Ne^{8+} is only $-0.000\,07$ a.u.[26] The second correction is the influence of relativistic effects on the correlation energy itself. It is our feeling that this effect will not alter the correlation energy any more than in the third significant figure, because this effect is expected to be significant only for the $1s$ states and the correlation diagrams involving $1s$ states contribute only 15% of the total correlation energy.

In Table XII, the total correlation energy from the present calculation is compared with the various variational calculations that have been discussed earlier in the section. Our result is listed with an error limit ± 0.01 a.u. This error limit is based on a consideration of the various limitations of our procedure that have been pointed out at different places in the text. Our results are in excellent agreement with both experiment and the most comprehensive variational calculation, namely, that of Bunge and Peixoto. The differences between our result and that of Viers *et al.* and Barr and Davidson are mainly due to the smaller range of l excitations that these authors utilized in their calculations. Nesbet, Barr, and Davidson's variational result included only the pair-excitations overshoots experiment. As pointed out earlier, this is a consequence of the fact that although the l convergence was well taken care of in this calculation, pair-pair correlations were not included. Nesbet's earliest result for the correlation energy is in surprisingly good agreement with experiment. As remarked already, this good agreement is due to the compensation of errors due to limitations in the range of l excitations and the absence of pair-pair interactions in Nesbet's calculation.

H. Concluding Remarks

It is gratifying that the perturbation and the variation approaches which are so different in their technical details and in over-all procedure, have given results which not only agree very well numerically with each other with respect to the correlation energy, but also provide similar conclusions about the role of various physical effects such as pair-pair interactions, l dependence of the multipole excitations, and many-particle effects. It is hoped that similar comparisons will be possible in the future in more complicated systems. The conclusions from this work and earlier CI calculations also suggest that if one is interested in the type of accuracy for the correlation energy that has been attained in neon, proper account has to be taken of pair-pair correlations and the l dependence of multipole excitations in pair correlations which require the inclusion of excited angular momentum states up to $l = 6$. Additionally, the comparison between various CI calculations among themselves, suggests that in such calculations, one has to be careful to incorporate substantial flexibility in the choice of one-electron radial functions, since choices of limited basis sets in neon have been found to give changes in the correlation energy by as much as 5%.

*Work supported by the NSF.

[1]K. A. Brueckner, Phys. Rev. 97, 1353 (1955).
[2]J. Goldstone, Proc. Roy. Soc. (London) A239, 267 (1957).
[3]J. D. Lyons and R. K. Nesbet, Phys. Rev. Letters 24, 433 (1970).
[4]R. K. Nesbet, Phys. Rev. A 2, 661 (1970).
[5]R. K. Nesbet, Phys. Rev. A 2, 1208 (1970).
[6]James E. Rodgers, C. M. Dutta, and T. P. Das, Phys. Rev. A (to be published).
[7]T. Lee, N. C. Dutta, and T. P. Das, Phys. Rev. Letters 25, 204 (1970).
[8]R. K. Nesbet, Phys. Rev. 155, 56 (1967).
[9]R. K. Nesbet, T. L. Barr, and E. R. Davidson, IBM Report on Atomic Physics RJ 610, No. 12457, 1969 (unpublished).
[10]Jimmy W. Viers, Frank E. Harris, and Henry F. Schaefer, Phys. Rev. A 1, 24 (1970).
[11]Terry L. Barr and Ernest R. Davidson, Phys. Rev. A 1, 644 (1970).
[12]Carlos F. Bunge and Eduardo M. A. Peixoto, Phys. Rev. A 1, 1277 (1970).
[13]Neil R. Kestner, Chem. Phys. Letters 3, 226 (1969).
[14]David A. Micha, Phys. Rev. A 1, 755 (1970).
[15]H. P. Kelly, Phys. Rev. 136, B896 (1964); 144, 39 (1966).
[16]H. P. Kelly, in *Advances in Theoretical Physics*, edited by K. A. Brueckner (Academic, New York, 1968).
[17]Edward S. Chang, Robert T. Pu, and T. P. Das, Phys. Rev. 174, 1 (1968); N. C. Dutta, C. Matsubara, R. T. Pu, and T. P. Das, *ibid.* 177, 33 (1969); T. Lee, N. C. Dutta, and T. P. Das, Phys. Rev. A 1, 995 (1970).
[18]The a.u. are Hartree a.u. in which the electron reduced mass in Ne is unity. Throughout our discussion, these units will be used.
[19]We have used Clementi's HF orbitals [Tables of Atomic Functions, IBM, 1965 (unpublished)] in generating our basis set.
[20]B. D. Day, Rev. Mod. Phys. 39, 719 (1967).

[21]Here "increase" means "increase in magnitude."
[22]V. Heine, Czech, J. Phys. B 13, 619 (1963).
[23]Charles W. Scherr, Jeremiah N. Silverman, and F. A. Matsen, Phys. Rev. 127, 830 (1962).
[24]Y. K. Kim, Phys. Rev. 154, 17 (1967).
[25]H. Hartman and E. Clementi, Phys. Rev. 133, A1295 (1964).
[26]C. L. Pekeris, Phys. Rev. 112, 1649 (1958).